RADAR: Road Obstacle Identification for Disaster Response Leveraging Cross-Domain Urban Data

LONGBIAO CHEN, Fujian Key Laboratory of Sensing and Computing for Smart Cities, Xiamen University
XIAOLIANG FAN, Fujian Key Laboratory of Sensing and Computing for Smart Cities, Xiamen University
LEYE WANG, Hong Kong University of Science and Technology
DAQING ZHANG, Institut Mines-Télécom, UMR 5157
ZHIYONG YU, Fuzhou University
JONATHAN LI, Fujian Key Laboratory of Sensing and Computing for Smart Cities, Xiamen University
THI-MAI-TRANG NGUYEN, University of Paris VI, UMR 7606, LIP6
GANG PAN, Zhejiang University
CHENG WANG*, Fujian Key Laboratory of Sensing and Computing for Smart Cities, Xiamen University

Typhoons and hurricanes cause extensive damage to coast cities annually, demanding urban authorities to take effective actions in disaster response to reduce losses. One of the first priority in disaster response is to identify and clear road obstacles, such as fallen trees and ponding water, and restore road transportation in a timely manner for supply and rescue. Traditionally, identifying road obstacles is done by manual investigation and reporting, which is labor intensive and time consuming, hindering the timely restoration of transportation. In this work, we propose RADAR, a low-cost and real-time approach to identify road obstacles leveraging large-scale vehicle trajectory data and heterogeneous road environment sensing data. First, based on the observation that road obstacles may cause abnormal slow motion behaviors of vehicles in the surrounding road segments, we propose a cluster direct robust matrix factorization (CDRMF) approach to detect road obstacles by identifying the collective anomalies of slow motion behaviors from vehicle trajectory data. Then, we classify the detected road obstacles leveraging the correlated spatial and temporal features extracted from various road environment data, including satellite images and meteorological records. To address the challenges of heterogeneous features and sparse labels, we propose a semi-supervised approach combining co-training and active learning (CORAL). Real experiments on Xiamen City show that our approach accurately detects and classifies the road obstacles during the 2016 typhoon season with precision and recall both above 90%, and outperforms the state-of-the-art baselines.

CCS Concepts: • **Human-centered computing** → *Ubiquitous and mobile computing systems and tools*;

Additional Key Words and Phrases: Mobility data mining, disaster response, cross-domain data, urban computing

Authors' addresses: Longbiao Chen, Fujian Key Laboratory of Sensing and Computing for Smart Cities, Xiamen University, longbiaochen@xmu.edu.cn; Xiaoliang Fan, Fujian Key Laboratory of Sensing and Computing for Smart Cities, Xiamen University; Leye Wang, Hong Kong University of Science and Technology; Daqing Zhang, Institut Mines-Télécom, UMR 5157; Zhiyong Yu, Fuzhou University; Jonathan Li, Fujian Key Laboratory of Sensing and Computing for Smart Cities, Xiamen University; Thi-Mai-Trang Nguyen, University of Paris VI, UMR 7606, LIP6; Gang Pan, Zhejiang University; Cheng Wang*, Fujian Key Laboratory of Sensing and Computing for Smart Cities, Xiamen University, cwang@xmu.edu.cn.

2474-9567/2017/12-ART130 $$15.00
https://doi.org/10.1145/3161159

ACM Reference Format:
Longbiao Chen, Xiaoliang Fan, Leye Wang, Daqing Zhang, Zhiyong Yu, Jonathan Li, Thi-Mai-Trang Nguyen, Gang Pan, and Cheng Wang*. 2017. RADAR: Road Obstacle Identification for Disaster Response Leveraging Cross-Domain Urban Data. *Proc. ACM Interact. Mob. Wearable Ubiquitous Technol.* 1, 4, Article 130 (December 2017), 23 pages. https://doi.org/10.1145/3161159

1 INTRODUCTION

Natural disasters, such as typhoons, hurricanes, and earthquakes, often bring extensive damage to city infrastructures and cause great loss of lives every year. With the rapid population growth and economic development, the cost of natural disasters have been constantly increasing in urban areas [5]. For example, on September 15, 2016, Typhoon Meranti made landfall in Xiamen City, China, leaving more than US$2.6 billion in economic losses[1]. In order to reduce human injuries and prevent further damage after natural disaster strikes, it is important for urban authorities to make efficient disaster response plans and take quick disaster response actions [38]. One of the first steps is to *restore road transportation*, such as cleaning fallen trees, draining ponding waters, and removing crashed vehicles on the road [24, 49]. These *road obstacles* may impede timely search and rescue, evacuation to shelters, and restoration of food and electric supply. Therefore, it is essential for urban authorities to identify and clear road obstacles in a timely manner.

Different strategies have been implemented to identify road obstacles for disaster response, such as sending out investigators to conduct road condition surveys, or reviewing traffic surveillance cameras to detect road obstacles from videos. The ability to accurately report *when, where, and what* types of obstacles are occurring on the road network is critical to the timely restoration of transportation. However, traditional strategies usually consume a great amount of human labor, which is especially expensive in disaster response scenarios, and thus hindering the timely report of road obstacles. Besides, sending out road investigators immediately after the disaster strikes may induce potential human injuries, and traffic surveillance cameras may be destroyed during the disaster, resulting in incomplete road obstacle reporting. Therefore, a *real-time, low-cost, and comprehensive* road obstacle identification method is in great need for disaster response.

Fortunately, with the advance of ubiquitous sensing technologies and paradigms, large amounts of urban sensing data are generated and collected in an unprecedented level [57, 61]. These *cross-domain heterogeneous urban sensing data* provide us with new opportunities to understand road conditions and identify potential road obstacles. In particular, two categories of urban sensing data are highly correlated with road conditions. The first category is *vehicle trajectory data*, which are generated by GPS-equipped vehicles (e.g., taxicabs) running on road surfaces [60]. These vehicles can be viewed as ubiquitous mobile sensors (i.e., *Vehicle-as-a-Sensor*, VaaS) constantly probing road conditions [63]. By analyzing the GPS trajectories of these vehicles, we can identify traffic anomalies potentially caused by road obstacles. For example, when a road segment is blocked by fallen trees, vehicles will not be able to go through it and their trajectories may vary from the normal patterns. The second category is *road environment data*, which describe the spatial and temporal environmental conditions of road segments, such as the road elevation, the roadside trees, and the weather conditions [56]. These road environment data can help infer the types of road obstacles after disaster strikes. For example, road segments with flourishing roadside trees may have higher probability of being blocked by fallen trees after a typhoon strike.

Therefore, we propose to leverage the above-mentioned cross-domain urban sensing data for automatic road obstacle detection and classification for disaster response. In the first step, we attempt to detect potential traffic anomalies caused by road obstacles. One intuitive approach is to extract a set of statistical traffic flow parameters (e.g., vehicle number) for each road segment from historical data. Then, one can build anomaly detection models to find significant and unusual decreases in traffic flow, and correspond these anomalies to the potential obstacles in

[1] https://en.wikipedia.org/wiki/Typhoon_Meranti

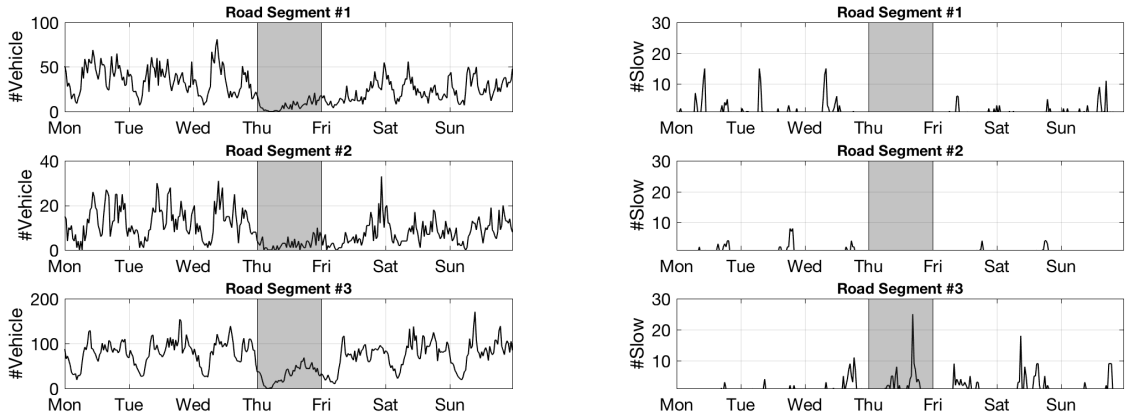

(a) Number of vehicles (#Vehicle)

(b) Number of slow motion behaviors (#Slow)

Fig. 1. Examples of traffic flow volumes and slow motion behaviors observed in three different road segments in Xiamen City from September 12, 2016 (Monday) to September 18, 2016 (Saturday). During the landfall of Typhoon Meranti on September 15, 2016 (Thursday), significant decreases of traffic flows are observed in all the three road segments, while only road segment #3 observe a significant increase of slow motion behavior.

the road segment. However, such a traffic-flow-based approach does not work well in disaster response scenarios. In fact, after a disaster strikes, the number of vehicles running on road usually decreases significantly due to safety concerns, generating abnormal traffic flows in almost every road segments. Consequently, the traffic anomalies caused by potential road obstacles are overwhelmed and thus difficult to detect. For example, in Figure 1(a), we observe significant decreases of traffic flow in all of the three road segments in Xiamen City after Typhoon Meranti's landfall, although only the third one is reported with road obstacles (fallen trees on Xianyue Road, the details are later presented in case studies).

In order to detect road obstacle from vehicle trajectories, we propose a novel approach by exploiting the *slow motion behaviors* in vehicle trajectories. Based on our observations, when a driver encounters road obstacles, they usually slow down the vehicle, observe the road conditions, and then make a decision to either change direction or slowly bypass the obstacle. Such slow motion behaviors can be extracted from vehicle GPS trajectories, and be exploited to detect potential road obstacles. For example, in Figure 1(b), we observe a significant increase of slow motion behaviors in road segment #3 after Typhoon Meranti's landfall on Xiamen City, which is induced by fallen trees on the road surface.

Nevertheless, it is still possible that some of the slow motion behaviors are not induced by road obstacles. For example, traffic lights at intersections may cause vehicles to slow down in a periodical pattern, and road segments with u-turn signs may also observe large number of slow-moving vehicles constantly. These kinds of slow motion behaviors, however, usually occur *regularly* on specific road segments, demonstrating certain spatio-temporal *patterns*. In contrast, the slow motion behaviors induced by road obstacles are usually *abnormal* in the given road segment and time span. Moreover, such an anomaly is usually observed in a *collective* way, i.e., impacting a collection of neighboring road segments and lasting for a consecutive period of time. For example, fallen trees in an intersection may cause unexpected slow motion behaviors in the surrounding roads until they

are removed. Therefore, we need to design an effective algorithm to separate the *collective anomalies of slow motion behaviors* for road obstacle detection.

After detecting the road obstacles, it is essential for urban authorities to identify their types, such as fallen trees, ponding water, and congested vehicles on road. Since different types of road obstacles may induce similar slow motion behaviors, it is difficult to classify these obstacles merely based on the vehicle trajectory data. Therefore, we propose to involve the road environment data to model the context of the obstacles, and thus inferring their corresponding types. For example, obstacles observed on flourishing road segments after a typhoon strike may probably be classified as fallen trees. To this end, the following challenges need to be addressed:

- *Heterogeneous features.* Due to the considerable variety and volume of road environment data, it is not straightforward to select a set of representative features to model the context of road obstacles. Moreover, how to effectively incorporate these heterogeneous features into a data analytics model is also challenging.
- *Insufficient labels.* In order to train a model for road obstacle classification, we need to collect a set of road obstacle instances as ground truth. However, validating road obstacles is labor-intensive and time-consuming, making it difficult to collect a large enough training set. Therefore, we need to propose an effective road obstacle classification model to learn from these sparse labels.

In this paper, we propose a two-phase framework for road obstacle detection and classification. In the first phase, we extract the slow motion behaviors from vehicle trajectories in each road segment, and build a spatio-temporal matrix to model these slow motion behaviors in a city-wide level. We then propose a *robust matrix factorization*-based method to separate the collective anomalies from the slow motion behavior matrix. To ensure that each separated anomalies are collective in neighboring road segments for a consecutive period of time, we incorporate a clustering-based outlier-remover method in the factorization algorithm, and detect road obstacles based on the corresponding collective anomalies. In the second phase, we identify two categories of contextual factors related to road obstacles from various road environment data, i.e., the *spatial contextual features* (e.g., roadside trees, road elevation, and road properties) and the *temporal contextual factors* (e.g., wind, rainfall, and visibility). In order to accurately classify the road obstacle with these heterogeneous features and sparse labels, we propose a semi-supervised learning approach combining co-training [39] with active-learning [45]. More specifically, we first train a spatial classifier and a temporal classifier, respectively, using the corresponding feature categories and a sparse training set. We then iteratively improve the model accuracy by adding the *confident* and *salient* instances in the unlabeled set to the training set, and retrain the model. A *confident* instance is identified if it receives the same label from both classifiers with high classification confidence [36], and a *salient* instance is identified if it is difficult to classify for both classifiers, i.e., receiving different labels with low confidence. We add the confident instances to the training set (co-training), and actively collect the labels of the salient instances from a crowdsensing platform (active learning), and add them back to the training set.

Briefly, the contributions of this paper include:

- To the best of our knowledge, this is the first work on road obstacle detection and classification for disaster response leveraging cross-domain urban sensing data. By fusing the large-scale vehicle trajectory data with the heterogeneous road environment data, we are able to accurately identify road obstacles for disaster response in a low-cost and automatic manner.
- We propose a two-phase framework to identify road obstacles by leveraging the slow motion behaviors and road environment contexts. In the detection phase, we exploit a sliding-window based method to extract slow motion behaviors from vehicle trajectories, and propose a cluster direct robust matrix factorization (CDRMF) approach to detect the collective anomalies induced by road obstacles from the spatio-temporal slow motion behavior matrix. In the classification phase, we extract two categories of road obstacle contextual features (i.e., spatial-features and temporal-features) from various road environment datasets, and propose a co-training and active learning (CORAL)-based approach to learn an effective classification

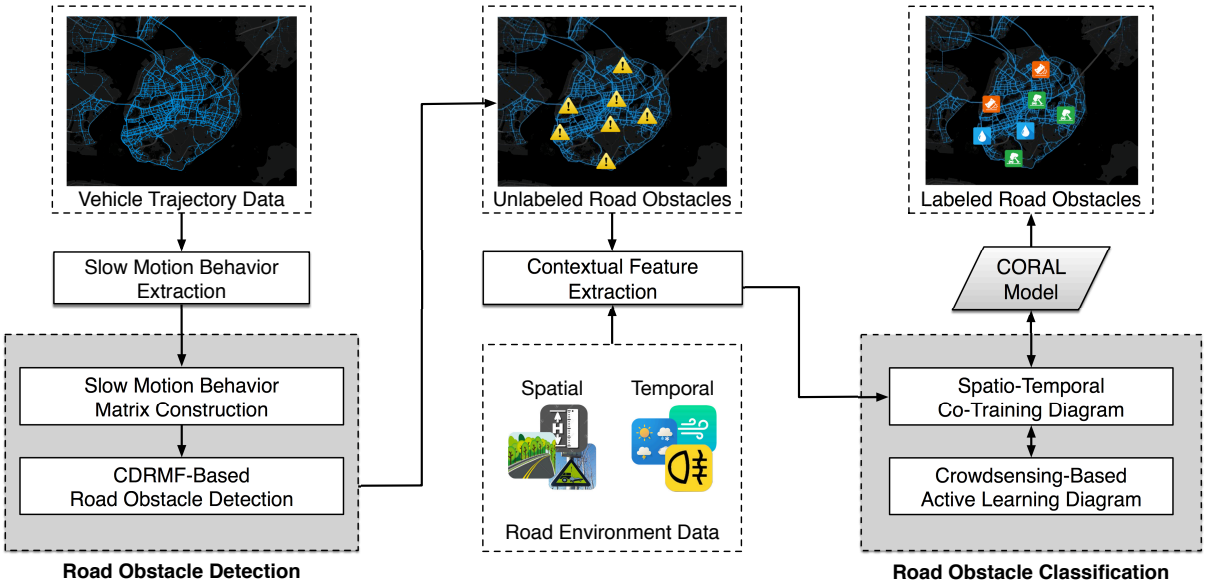

Fig. 2. Overview of the framework.

model using the spatio-temporal features and a sparse training set. The CORAL approach iteratively improves the classification accuracy by adding confident instances to the training set, and actively labeling salient instances using a crowdsensing platform.

- We evaluate our framework on Xiamen City with a large-scale taxi trajectory dataset and various environment sensing datasets. Results show that our framework accurately detects and classifies different types of road obstacles during the 2016 typhoon season, achieving an overall precision and recall both above 90%, and outperforms the state-of-the-art baseline methods.

2 PRELIMINARY AND FRAMEWORK OVERVIEW

Definition 2.1. **GPS Dataset**: the vehicle GPS dataset we collect can be described by a set of GPS points denoted by 4-tuples:

$$P = \{p | p = (v, t, lat, lng)\}$$

where v, t, lat, lng are the unique vehicle ID, time stamp, latitude, and longitude from GPS transmitters.

Definition 2.2. **Vehicle Trajectory**: we define a vehicle trajectory as a sequence of GPS points $p_1 \rightarrow p_2 \rightarrow \cdots \rightarrow p_n$, where $p_i \in P, 1 \leq i \leq n$.

Definition 2.3. **Road Segment**: we partition a city into an $I \times J$ grid map based on the longitude and latitude, and define a road segment r as a grid containing roads for vehicles.

Definition 2.4. **Time Span**: we divide the duration of observation data into equal time spans t, each time span lasts for a period of time, e.g., half an hour.

We propose RADAR, a two-phase framework to detect and classify road obstacles for disaster response. As shown in Figure 2, we first extract slow motion behaviors from a large-scale vehicle GPS trajectory dataset with a sliding-window-based method. In the road obstacle detection phase, we organize the slow motion behaviors

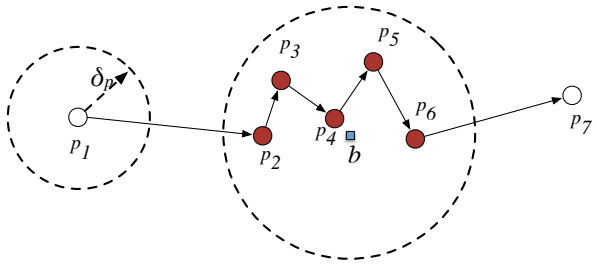

Fig. 3. Slow motion sequence extraction from GPS trajectory leveraging an adaptive sliding-window.

into a spatio-temporal matrix with a road segment dimension and a time span dimension. We then perform the CDRMF algorithm on the matrix to extract collective anomalies of slow motion behaviors, and correspond these anomalies to the potential road obstacles. In order to classify these detected road obstacles, we identify several relevant environment sensing data, and extract a set of spatial and temporal contextual features correspondingly. In the road obstacle classification phase, we exploit the co-training diagram to train a spatial classifier and a temporal classifier, respectively, using the corresponding contextual features and a sparse training set. We iteratively add confident and salient unlabeled instances to the training set to improve the model accuracy, leveraging a crowdsensing-based active learning diagram which actively collect labels for the salient instances from a crowdsensing platform. We elaborate the key steps of the framework in the following sections.

3 SLOW MOTION BEHAVIOR EXTRACTION

The slow motion behaviors of vehicles may indicate potential obstacles on the road. For example, fallen trees that block a road may force the drivers to slow down and change direction. Such slow motion behaviors can be captured from vehicles' GPS trajectories if the data points are collected frequently enough. In this work, we use a taxi GPS trajectory dataset collected every one minute. We elaborate on the method to extract slow motion behaviors from taxi trajectories as follows.

First, we employ an adaptive sliding-window-based method [15] to extract slow motion sequences from taxi GPS trajectories. More specifically, for a trajectory $p_1 \rightarrow p_2 \rightarrow \cdots \rightarrow p_n$, we extract every slow motion sequence $p_m \rightarrow p_{m+1} \rightarrow \cdots \rightarrow p_{m+k} (1 \leq m < n, 1 \leq k \leq n-m)$ in which the distance ($dist$) between each pair of adjacent points is less than a threshold δ_p, i.e.,

$$\forall m \leq i < m+k, dist(p_i, p_{i+1}) < \delta_p \tag{1}$$

We use a sliding-window with adaptive size along the trajectory to find such slow motion sequences. In particular, we dynamically extend the window size by adding new points until the newly-formed sequence violates requirement 1. We use an example in Figure 3 to elaborate on the process. For the trajectory $p_1 \rightarrow p_2 \rightarrow \cdots \rightarrow p_7$, we start by creating a window consisting of the first two points (p_1, p_2 in this case), and check whether the distance between p_1 and p_2 is less than δ_p. Since $dist(p_1, p_2) > \delta_p$, we discard this window, and slide the window to start over from the end point (p_2), and create a new window (p_2, p_3). We see $dist(p_2, p_3) < \delta_p$ so the window is kept; since $dist(p_3, p_4) < \delta_p$, we extend the window by adding p_4, and repeat this procedure for the next adjacent points until the distance constraint is violated. Finally, we obtain a sequence containing a set of consecutive points $p_2 \rightarrow \cdots \rightarrow p_6$.

We filter out sequences with long-term duration, which may correspond to non-driving behaviors such as taxi driver shift or vehicle repair. Finally, we map each slow motion sequence $p_m \rightarrow p_{m+1} \rightarrow \cdots \rightarrow p_{m+k}$ to a slow

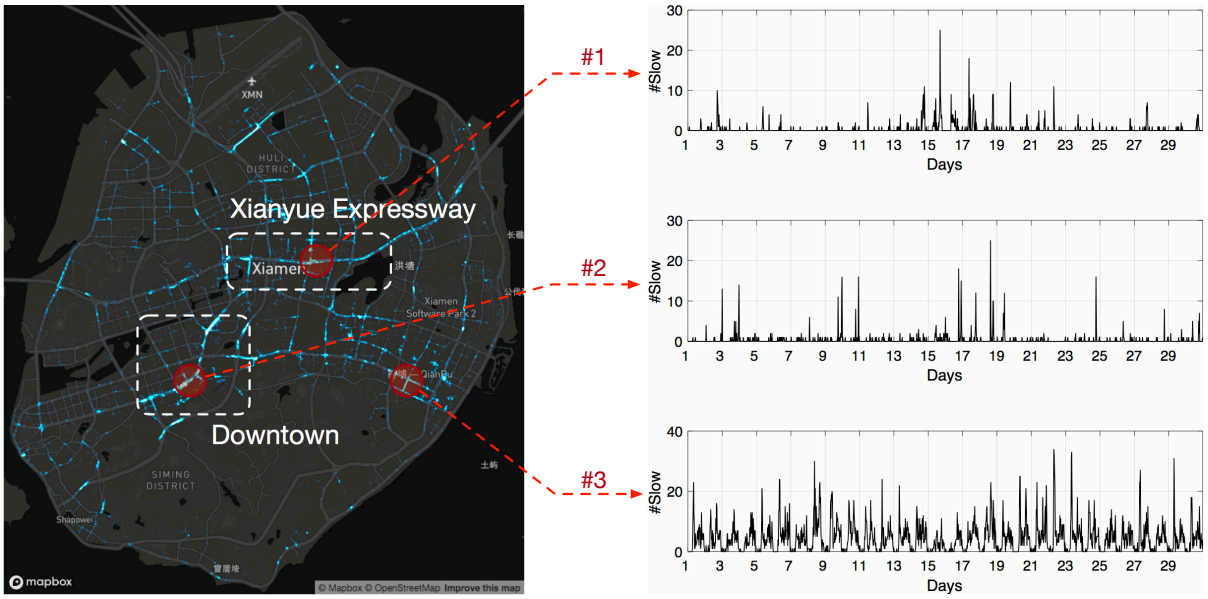

(a) Visualization of extracted slow motion behaviors

(b) Temporal variations of three typical road segments

Fig. 4. An illustrative visualization of the extracted slow motion behaviors after the landfall of Typhoon Meranti in Xiamen City (2016/09/15 09:00–2016/09/15 17:00), and the temporal variations of slow motion behaviors in three typical road segments during one month (2016/09/01–2016/09/30). (#1: Xianyue Expressway, #2: Hubin South Road, #3: Qianpu East Road)

motion behavior, as denoted by a triple:

$$b = (v, r, t)$$

where v is the corresponding vehicle ID. We determine the road segment r by mapping the coordinates of the sequence centroid $[(p_m.lat + p_{m+k}.lat)/2, (p_m.lng + p_{m+k}.lng)/2]$ to the city grid system, and determine the time span t by mapping the middle of the duration $(p_m.t + p_{m+k}.t)/2$ to the time span partition system.

Figure 4(a) shows a visualization of the extracted slow motion behaviors after the landfall of Typhoon Meranti in Xiamen. We observe a cluster of slow motion behaviors on the major roads of the downtown area, which may be induced by ponding water on the road surface, since the elevation of downtown Xiamen is relatively low[2]. Another cluster of slow motion behaviors can be found along the Xianyue expressway, which was covered by flourishing trees, and the slow motion behaviors may be induced by fallen trees during the typhoon landfall.

4 ROAD OBSTACLE DETECTION

In this phase, our objective is to detect road obstacles from the extracted slow motion behaviors. The rationale behind this approach is that when an obstacle is present in a road segment, it may induce a *collective anomaly* [64] of slow motion behaviors. The meaning of *collectiveness* is two-fold. First, such an anomaly may be observed in a collection of neighboring road segments. Second, such an anomaly may last for a consecutive period of time after the road obstacle is present. For example, when fallen trees block a lane, various slow motion behaviors, such as turning and bypassing, can be observed in the surrounding road segments and last for a period of time until the road obstacle is removed. Consequently, simply building a time series anomaly detection [6] model for

[2]http://www.floodmap.net/elevation/ElevationMap/?gi=1790645

each road segment to detect road obstacle does not work well in this problem, as the *spatio-temporal collectiveness* is not properly preserved and modeled.

The second challenge is that the slow motion behaviors we collect are in a *mixed* state due to various causal factors. Based on our observations, slow motion behaviors can be induced not only by road obstacles, but also by traffic lights and turning signs, rush hour traffic congestions, picking up and dropping off passengers, etc. Directly detecting anomalies from such a mixed state and corresponding them to road obstacles can be very difficult and unreliable [13, 21].

To address these challenges, we propose a robust matrix factorization-based approach to separate the spatio-temporal collective anomalies from the mixed slow motion behaviors, and correspond them to the road obstacles. First, we build a slow motion behavior matrix with a road segment dimension and a time span dimension. Each cell of the matrix denotes the number of slow motion behaviors observed in the specific road segment during the specific time span. Then, we separate the slow motion behaviors induced by different causal factors based on their spatio-temporal properties. We note that slow motion behaviors induced by traffic lights and turning signs are usually observed *regularly* in some specific road segments and time spans, while the collective anomalies of slow motion behaviors induced by road obstacles tend to be *abnormal* events in the spatio-temporal space. Moreover, such collective anomalies are usually observed in geographically *clustered* road segments over a *consecutive* period of time. With these insights, we propose a *Cluster Direct Robust Matrix Factorization (CDRMF)* [3, 54] approach to automatically decompose the mixed slow motion behavior matrix into a *low-rank* component and a *sparse-and-clustered* component. The low-rank component represents the regular slow motion behaviors induced by traffic lights and turning signs, etc., while the sparse-and-clustered component corresponds to the unusual and clustered collective anomalies induced by road obstacles. We elaborate on the details of our approach as follows.

4.1 Slow Motion Behavior Matrix Construction

We build a spatio-temporal matrix $M \in \mathbb{R}^{N_r \times N_t}$ with two-dimensions denoting N_r road segments and N_t time spans. Each entry of the matrix $M(r, t)$ denotes the number of slow motion behaviors observed in road segment r during time span t.

In particular, we analyze the temporal variations of slow motion behaviors in three typical road segments in Xiamen City during one month (September 2016), as shown in Figure 4(b). For road segment #1 (Xianyue Expressway), we observe a significant increase of slow motion behaviors during Typhoon Meranti's landfall in Xiamen (September 15–17), which corresponds well with the fact that fallen trees induced by strong winds block several lanes in Xianyue Expressway[3]. We also observe several abnormal increases of slow motion behaviors in road segment #2 (Hubin South Road), which is built in a low elevation area. These anomalies might be correlated with the road surface water ponds induced by heavy rains. As an counter example, we observe regular patterns of slow motion behaviors on road segment #3 (Qianpu East Road), which is a popular business and activity district in Xiamen City, and thus the regular patterns may correspond to the passenger pick-up and drop-off events instead of road obstacles.

4.2 CDRMF-Based Road Obstacle Detection

With the slow motion behavior matrix M constructed, we then need to separate the regular and anomalous slow motion behaviors apart. Such a problem can be addressed by matrix decomposition techniques [32] by imposing structural constraints on the decomposed components [29]. In particular, Robust Matrix Factorization (RMF) [3, 29, 54] approaches have been proposed to decompose a mixed matrix into a low-rank part and a sparse part in an automatic manner, and have been widely adopted in robust modeling and anomaly detection [47]. The low rank component can be used to describe the regular patterns of slow motion behaviors, but the sparse

[3] http://weibo.com/1976447603/E8vIamwnv

component may have arbitrary structure which does not necessarily correspond to the collective anomalies we desire. Therefore, we improve the RMF approach by adding a clustering step to pursue a sparse-and-clustered component that corresponds to the collective anomalies.

Problem: we define our objective as to decompose the mixed matrix M into a low-rank matrix L and a sparse-and-clustered matrix S, i.e.,

$$\begin{aligned} & M = L + S \\ s.t. \quad & rank(L) \leq k, \\ & card(S) \leq c, \\ & outlier(S) \leq \epsilon \\ & L \geq 0, S \geq 0 \end{aligned} \tag{2}$$

where $card(S)$ denotes the cardinality of S, i.e., the number of non-zero elements in S. By imposing the constraints on $rank(L)$ and $card(S)$, we pursue a low-rank L and a sparse S, respectively. Besides, we need to make sure that the non-zero elements in S are distributed collectively in neighboring road segments and consecutive time spans. Therefore, we use $outlier(S) \leq \epsilon$ to prevent outliers that are isolated from their spatio-temporal neighbors, where ϵ is a very small value close to zero.

Solution: solving Problem (2) is not trivial due to its non-convex constraints [54]. Traditionally, such kind of problem is solved using relaxation techniques [47], i.e., by relaxing the matrix rank of L with its nuclear norm [47], and relaxing the cardinality of S using its ℓ_1 norm [48]. The relaxed problem is then solved using alternating minimization techniques [47]. However, the traditional relaxation techniques have several limitations. First, it is difficult to represent and impose the clustered structure of S to the relaxation problem. Second, it is unknown how well the relaxation approximate the original problem in general [54].

In this work, we proposed a Clustered Direct Robust Matrix Factorization (CDRMF) approach for collective anomaly detection, which is built on the recently proposed Direct Robust Matrix Factorization (DRMF) method [54]. Instead of using relaxation techniques, the DRMF approach directly solves the matrix decomposition problem by alternatively optimizing the low-rank component and the sparse component. In order to impose the clustered structure constraint, we improve the DRMF algorithm by iteratively removing the isolated outliers in the sparse component in the optimization process.

Algorithm: the detailed process of CDRMF is described in Algorithm 1. The CDRMF algorithm is initialized with the mixed matrix m, the rank constraint k, and the cardinality constraint c. In each iteration, we perform two steps to update the low-rank component L and the sparse-and-clustered component S. In the first step, we fix and remove the sparse component S from M, and approximate $M - S$ by a low-rank component L. In the second step, we fix and remove the low-rank approximation L from M to obtain the residual $M - L$, and find the optimal sparse-and-clustered S to recover the residual. We repeat the process until the algorithm is converged or the maximum iteration number is reached. Finally, we output the low-rank component L as the regular patterns, and the sparse-and-clustered component S as the collective anomalies.

In order to solve the low-rank approximation problem, we perform Single Value Decomposition (SVD) [26] on $M - S$, and truncate its top-k singular vectors to construct a rank-k approximation $L = M - S$. Since only the first k singular vectors are required, we accelerate the computation using partial SVD algorithms [55]. We propose a two-step approach to solve the sparse-and-clustered optimization problem. First, we find the optimal approximation of the residual $M - L$ under the cardinality constraint $card(S) \leq c$. This can be done directly by copying the top-c largest values in $M - L$ to S and setting the rest entries of S to zeros. The proof of this method can be found in [54] and thus omitted here. Then, we perform a clustering operation for the non-zero elements in S using the DBSCAN algorithm [44], and remove the outliers that are isolated from their spatio-temporal neighbors. In particular, we use the geographic distance between road segments and temporal distance between time spans

to determine the search distance in clustering. In this way, we obtain a sparse-and-clustered component S to approximate the residual in the iteration.

ALGORITHM 1: The CDRMF algorithm for collective anomaly detection

Input: M the slow motion behavior matrix
k the maximum rank
c the maximum cardinality
max_iter the maximum number of iterations
Output: L the low-rank component
S the sparse-and-clustered component

Initialize: $S \leftarrow \mathbf{0}$
while *not converged and iteration* < max_iter **do**
  a) Solve the low-rank approximation problem:
    $L = \arg\min_L ||A - L||_F, \quad A = M - S$
    $s.t. \quad rank(L) \leq k$
  b) Solve the sparse-and-clustered optimization problem:
    $S = \arg\min_S ||B - S||_F, \quad B = M - L$
    $s.t. \quad card(S) \leq c, \quad outlier(S) \leq \epsilon$
  $error \leftarrow ||M - L - S||_F$
end

4.3 Road Obstacle Detection

Finally, we map the detected sparse-and-clustered collective anomalies to the potential road obstacle event. We note that one road obstacle may induce several collective anomalies spanning among neighboring road segments and lasting for a consecutive period of time. In particular, we assign each cluster in S with a label and use the cluster to denote the road obstacle event e , i.e.,

$$e_i = \{(r, t)|S(r, t).label = i\}$$

5 CONTEXTUAL FEATURE EXTRACTION

With the road obstacles detected, our next objective is to recognize the types of these obstacles, such as fallen trees and ponding water. However, since different types of obstacles may induce similar slow motion behaviors, it is rather difficult to distinguish different types of road obstacle merely based on vehicle trajectory data. Therefore, we propose to incorporate the cross-domain environment sensing data to model the context of the road obstacles, and then infer their corresponding types base on the contextual features.

However, due to the considerable variety and volume of these road environment sensing data, it is still not trivial to identify the correlated factors and extract the effective features for road obstacle classification. Therefore, we conduct a series of empirical studies to analyze the correlations between road obstacles and various environment contextual factors, leveraging a set of road obstacle events and road environment datasets collected from Xiamen City. We elaborate the details of analysis as follows.

5.1 Spatial Contextual Factors

Based on previous studies and surveys [34, 52], the geographic environment conditions of a road segment can provide strong evidence for inferring the types of potential road obstacles. For example, road segments with flourishing trees may have higher probability of being blocked by fallen trees after strong winds, and low-elevation

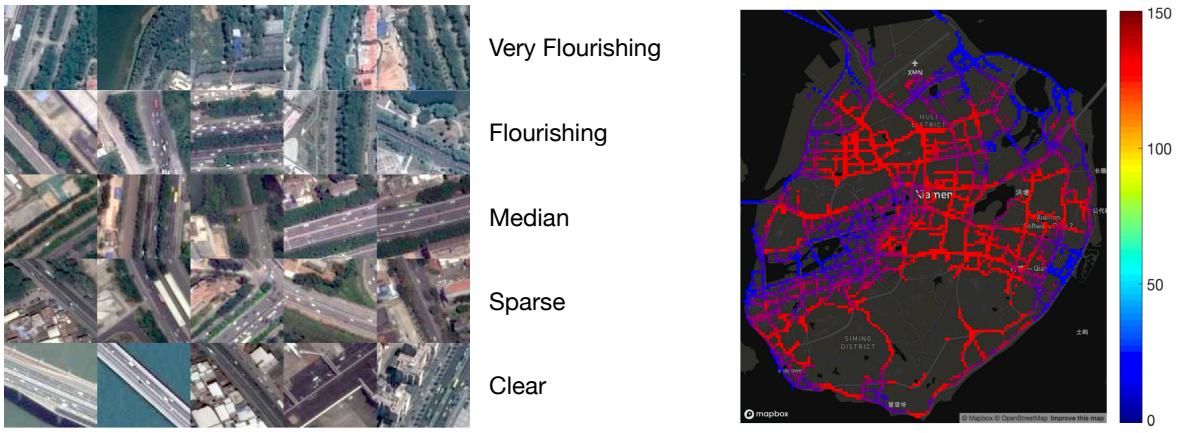

(a) Roadside tree coverage labeling sample results

(b) Road segment elevation map (in meters)

Fig. 5. Illustrative results of road environment contextual feature extraction.

road segments may be more vulnerable to heavy rains. In particular, we identify the following three key spatial contextual factors and extract a set of features from the corresponding road environment data.

Roadside tree coverage: the conditions of roadside trees can be observed from high-definition satellite images. However, labeling the degree of tree coverage for thousands of road segments requires great human effort. Therefore, we employ a deep learning-based approach [33] to automatically label roadside tree coverage. First, we obtain a set of satellite images I from Google Earth[4], and randomly select a small subset of road segment images I_t as training examples. Then, we manually label the degree of roadside tree coverage for the training examples into five categories, *very flourishing, flourishing, median, sparse, clear*. Some examples of the labeled images can be seen in Figure 5(a). Finally, we use a pre-trained deep learning network, AlexNet [30], to extract features from the set of unlabled road segment images $I - I_t$, and predict their corresponding labels using a SVM classifier [8]. Some examples of the predicted labels are also present in Figure 5(a).

Road segment elevation: road segments with low elevation may be vulnerable to heavy rains caused by typhoons and hurricanes. The elevation of road segments can be obtained from various Digital Elevation Model (DEM) [43] data sources with different resolutions. In this work, we extract road segment elevation data from Google Earth, which provides a base resolution of 30 meters [43] in Xiamen City. An extracted elevation map for all the road segments in Xiamen City is shown in Figure 5(b).

Road segment properties: road obstacles, such as crashed vehicles caused by traffic accidents and congested vehicles caused by malfunctioning traffic lights, tend to be observed in road segments with complicated conditions, e.g., road intersections, traffic circles, and tunnel entries and exits. We identify these complicated road segments and use this prior knowledge as a feature to infer traffic-induced road obstacles. In particular, we label the road segment properties by the following categories: *intersection, circle, tunnel entry/exit, none*. We retrieve the locations of road interactions and circles from Xiamen Traffic Police, and manually label the locations of tunnel entries/exits.

[4]https://www.google.com/earth/

5.2 Temporal Contextual Factors

In a road segment, different types of obstacles may occur under different temporal contexts [20, 51]. For example, fallen trees are usually caused by strong winds, water ponds on road faces are usually formed after heavy rains, and vehicle congestion and accidents are reported more frequently when drivers have limited visibility. By exploiting the meteorological data from the Weather Underground API[5] and Xiamen Meteorological Bureau[6], we identify the following temporal contextual factors and extract a set of corresponding features.

Wind speed: since fallen trees are usually observed after strong winds with a delay, we extract the wind speed one hour before for each obstacle as the contextual feature, measured in m/s.

Rain precipitation: similarly, water ponds are usually formed after heavy rains. Therefore we extract the rain precipitation one hour before for each road obstacle as the corresponding contextual feature, measured in centimeters.

Road visibility: visibility may greatly impact driving safety, especially in heavy rains and foggy weather. Limited visibility in a road segment may cause potential risks of traffic accidents and congestions, especially in complicated road segments. We extract fine-grained visibility data in each road segment as the corresponding contextual feature, measured in meters.

6 ROAD OBSTACLE CLASSIFICATION

In this phase, our objective is to classify the detected road obstacles based on the extracted contextual features. Intuitively, we can train a predictive model (e.g., artificial neural networks) to classify the road obstacles using the various contextual features. However, since the spatial and temporal features are extracted from heterogeneous sources and vary significantly in scales, equally treating these features does not work well in our problem [62]. The other challenge is that obtaining a set of labeled road obstacles large enough for training a predictive model is rather difficult, since road obstacle reporting is still labor intensive and time consuming, especially in disaster response scenarios.

In order to address the challenges of heterogeneous features and insufficient labels, we propose a semi-supervised learning approach combining co-training with active-learning (CORAL). Co-training is a multi-view learning technique that leverages two conditionally independent models to predict the target labels, and use the confident prediction results to further improve the model accuracy in an iterative manner [39, 62]. We group the heterogeneous features into two sets, i.e., spatial and temporal feature sets, and input these features into the co-training framework. Active-learning takes another approach to improve prediction accuracy by dynamically selecting a set of uncertain predictions and asking the users to provide labels for these instances, and then it feeds them back to retrain the model iteratively [50, 59]. We propose a crowdsensing-based platform to obtain a relatively small set of training labels, and use the active-learning mechanism to gradually obtain new labels during the training process. The design diagram of the CORAL approach is illustrated in Figure 6. We elaborate on the details as follows.

6.1 The Co-Training Paradigm

In the co-training paradigm, we feed the two categories of contextual features into a spatial and temporal inference model, respectively, and iteratively add the instances with high prediction confidence to the training set to improve model accuracy.

More specifically, we denote the set of detected road obstacles as $G = \{G_1, G_2\}$, where G_1 is the small initial set of labeled obstacles, and G_2 is the large unlabeled set. We obtain the labels of G_1 by leveraging a crowdsensing-based platform, which is detailed in the evaluation section. Using the set of spatial features F_s and temporal

[5] https://www.wunderground.com/weather/api/
[6] http://www.xmqx.gov.cn

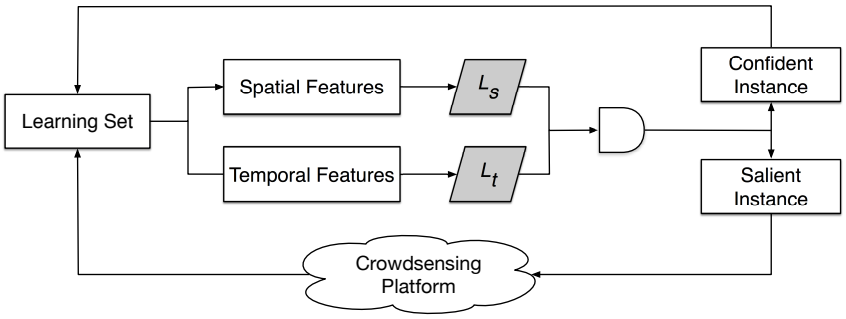

Fig. 6. The learning diagram of the proposed CORAL model.

features F_t, we train a spatial learner L_s and a temporal learner L_t respectively, i.e.,

$$L_s \leftarrow L_s.learn(F_s, G_1) \qquad L_t \leftarrow L_t.learn(F_t, G_1) \tag{3}$$

Afterward, we apply L_s and L_t to each instance of G_2, and select N_c instances that receive the same label from both L_s and L_t with highest confidence, respectively. Finally, we add the selected instances to G_1 as labeled instances. We repeat this process until G_2 is empty or a maximum number of iterations is reached.

6.2 The Active Learning Paradigm

Ideally, the co-training paradigm can improve the model accuracy with the confident unlabeled instances. However, this approach does not ensure that the selected confident instances are always valuable for improving the predictive capability of the model [59]. In other words, we can directly select some *salient* instances to the models to improve their accuracy. To this end, we incorporate a active learning process to the co-training diagram.

More specifically, in each iteration, after applying L_s and L_t to each instance of G_2, we further select N_a instances that are considered most difficult to predict for both predictors. In particular, we select instances that receive different labels from L_s and L_t with lowest confidence. We then use the crowdsensing platform to collect the labels for these instances. Finally, we add these salient labeled instances to G_1 and retrain the models using the co-training paradigm.

6.3 Online Learning and Classification

The CORAL model works in a online manner so that learning and classification can be achieved simultaneously. More specifically, we maintain a learning set G for training the classification model using the CORAL model. Given a new road obstacle e and the label set $C = \{c_1, c_2, \ldots, c_l\}$, we apply the learned L_s and L_t on e separately, and determine the final label c by the product of the two confidence scores generated by the two learners, defined as follows:

$$c = \arg\max_{c_i \in C} \quad P_s(C = c_i) \times P_t(C = c_i) \tag{4}$$

where P_s and P_t are the predicted probabilities of the spatial and temporal learners, respectively. After that, we append e to the training set G and retrain the CORAL model. If additional labels are required during the retraining, the corresponding crowdsensing platform tasks will be allocated and completed in a given time constraint. Since online model updating is frequently performed, we adopt a naïve Bayesian network [25] as the ideal multi-class classifier for the learners L_s and L_t, which is highly scalable, easy to train, and outputs the desired classification probabilities for confidence estimation.

7 EVALUATION

In this section, we first introduce the experiment settings, and then present the evaluation results on road obstacle detection and recognition. We also conduct a series of case studies to demonstrate the effectiveness of our method.

7.1 Experiment Settings

7.1.1 Datasets

We evaluated our framework in Xiamen City during the 2016 Pacific typhoon season[7]. Xiamen is a coastal city which suffers from an average of 4–5 times of typhoon each year. We collected a large scale taxi GPS trajectory dataset and various road environment datasets from July 2016 to December 2016, as summarized in Table 1. The dataset details and pre-processing steps are elaborated as follows.

Taxi GPS trajectory data: we obtained a large-scale taxi GPS trajectory dataset from Xiamen Traffic Police. The dataset contains GPS trajectories of 5,486 taxis reported every 1 minute. We extracted only trajectories data points in the metropolitan area (i.e., Xiamen Island) during the second half year of 2016.

Road environment data: we partitioned Xiamen City into $100m \times 100m$ grids, and obtain 154×136 grids. We then extracted grids with vehicle density above average as road segments for vehicles, obtaining 3,928 road segments in total. Upon this basis, we collected a set of satellite image patches and elevation data for each road segment from Google Earth for roadside tree coverage labeling and road elevation sensing, respectively. We also compiled an hourly meteorology dataset for each road segment, containing the wind speed, rain precipitation, and visibility readings, based on the data from the Weather Underground API and Xiamen Meteorological Bureau.

Road obstacle data: we developed a crowdsensing platform to collect road obstacles during typhoon seasons, as shown in Figure 7. We recruited 10 participants to finish the crowdsensing tasks, and each task was assigned randomly to three participants for cross-validation to avoid observer bias. Each participant was asked to report the time, location, and type of the road obstacle along with the source materials such as images and videos. An important source is the social media accounts of urban authorities and local news agencies, such as the Weibo[8] accounts of Xiamen Traffic Police[9] and Xiamen News Network[10]. Besides, the traffic congestion and accident records provided by Xiamen Traffic Police were used as another important source to identify congested and crash vehicles on the road. Based upon the crowdsensing platform, we collected a total number of 159 road obstacle events from July 2016 to December 2016. We use this dataset as the ground-truth for evaluating the performance of various road obstacle detection and classification methods.

7.1.2 Evaluation Plan

We evaluated the performance of our framework in an online manner. We first extracted taxi slow motion behaviors in all the road segment once every 30 minute. For road obstacle detection, we maintained a slow motion behavior matrix M with a time window of one month, i.e., $2 * 24 * 30 = 1440$ time spans, and updated the matrix when data from a newer time window were collected. We performed the CDRMF algorithm on M to detect a set of road obstacles $\{e_i\}$, and compared the detection results with the ground truth dataset. For road obstacle classification, we maintained a learning set G and incrementally add new instances into the set. Specifically, for each newly detected road obstacle $\{e_i\}$, we used the learned CORAL model to classify it, and then add $\{e_i\}$ to the training set and update the CORAL model. The initial labels and the additional labels required during the model updating were obtained by dynamically allocating crowdsensing tasks to the participants. Finally, we compared the overall classification results with the ground truth dataset to evaluate the model accuracy.

7.1.3 Evaluation Metric

[7] https://en.wikipedia.org/wiki/2016_Pacific_typhoon_season
[8] Weibo is a Twitter-like social network popularly used in China.
[9] http://weibo.com/fjxmjj
[10] http://weibo.com/xmnn

Table 1. Summary of Datasets

Data type	Item	Value
Vehicle trajectory data	# Taxis	5,486
	Sampling rate	every minute
Road environment data	# Road segments	3,928
	Satellite image resolution	2.5 meter
	Elevation resolution	30 meter
	Meteorology data	every hour
Road Obstacles	# Fallen trees	71
	# Ponding water	54
	# Congested and crashed vehicles	34
Data collection period	07/01/2016 00:00–12/31/2016 23:59	
Geographic coverage area	Southwest: [24.423250, 118.064743], Northeast: [24.561485, 118.198504]	

We compared the detected road obstacles with the ground truth dataset to evaluate the accuracy of a detection method. Specifically, if a detected obstacle is found in the ground truth dataset, we call it a *true positive (TP)*, and otherwise a *false positive (FP)*. For a true road obstacle that is not detected using the detection method, we call it a miss, or *false negative (FN)*. With these definitions, we adopted the following metrics to quantitatively evaluate the performance of the detection method:

$$precision = \frac{|TP|}{|TP| + |FP|}, \quad recall = \frac{|TP|}{|TP| + |FN|}, \quad F1\text{-}Score = \frac{2 \cdot precision \cdot recall}{precision + recall} \tag{5}$$

We employed the similar metrics to evaluate the performance of the multi-class road obstacle classification method. Specifically, we organized the classification results into a confusion matrix [23] C, where each row of the matrix represents the instances in a predicted class and each column represents the instances in a ground truth class. Each element $C_{i,j}$ counts the number of road obstacles that are predicted as class i while actually are in class j. With these definitions, we derived the following metrics:

$$precision = \frac{C_{i,i}}{\sum_j C_{ij}}, \quad recall = \frac{C_{i,i}}{\sum_j C_{ji}}, \quad F1\text{-}Score = \frac{2 \cdot precision \cdot recall}{precision + recall} \tag{6}$$

We can see that (5) is a special case of (6).

7.1.4 Baseline Methods

We compared our method with various baseline methods with regard to road obstacle detection and classification. For road obstacle detection, we compared our CDRMF method with the following baselines:

TFBOY: the traffic-flow-based anomaly detection (TFBOY) baseline method directly uses the number of vehicles in each road segment during each time span to construct a traffic flow matrix, and use the same matrix decomposition approach for road obstacle detection.

ARIMA: the single-road-segment time-series-based baseline method models the number of slow motion behaviors in each road segment as a time series, and employs an auto-regressive integrated moving average (ARIMA) model [7] to detect significant and unusual events as potential road obstacles.

DRMF: this baseline method differs from the proposed CDRMF method in that it does not perform a clustering step to remove isolated anomalies.

For road obstacle classification, we compare our CORAL method with the following baselines:

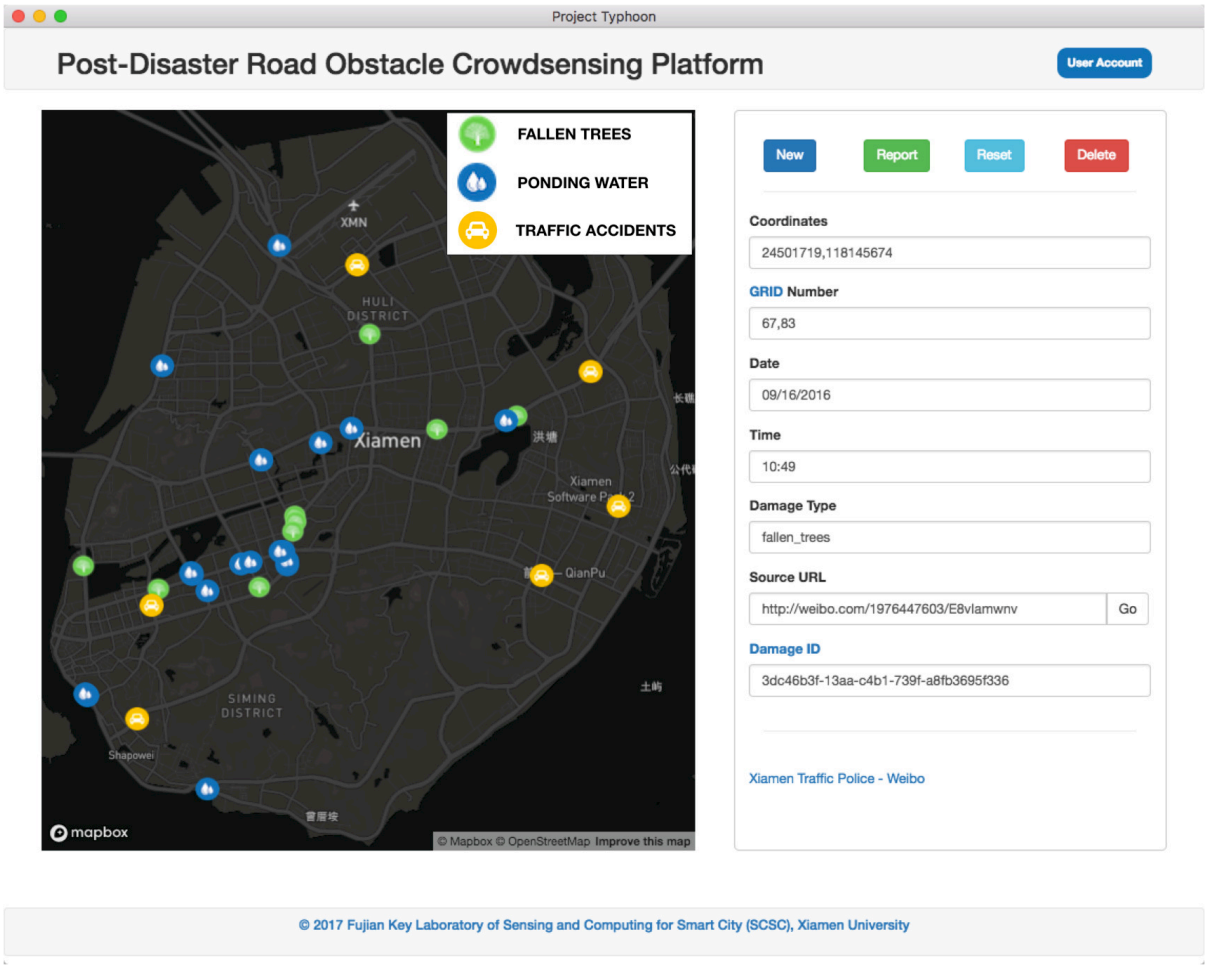

Fig. 7. The developed crowdsensing platform for collecting road obstacles.

ST-ANN: this baseline method directly concatenate the spatio-temporal contextual features, and uses all the instances in the training set to train an Artificial Neural Network (ANN) model for road obstacle classification.

SCAL: this baseline method exploits only the spatial contextual (SC) features to build a road obstacle classifier using a naive Bayesian network. The active learning (AL) diagram is also exploited to train the model iteratively from a minimal training set.

TCAL: similarly, this baseline method exploits the temporal contextual (TC) features and active learning (AL) to build a road obstacle classifier by iteratively training a naive Bayesian network with a minimal training set.

COTA: this baseline method uses the co-training diagram (COTA) alone without active learning. It trains a naive Bayesian network-based spatio-temporal model and iteratively improves the model accuracy using confident unlabeled data.

In order to achieve fair comparison, we make sure that the size of the initial label set and the number of labels finally used in each active learning-based baselines (including SCAL, TCAL, and CORAL) are the same.

Table 2. Road obstacle detection results

Methods	Precision	Recall	F1
TFBOY	0.503	0.489	0.496
ARIMA	0.872	0.697	0.775
DRMF	0.730	0.906	0.809
CDRMF	0.953	0.931	0.942

Table 3. Road obstacle classification results

Methods	Precision	Recall	F1
ST-ANN	0.921	0.956	0.938
SCAL	0.772	0.738	0.755
TCAL	0.691	0.649	0.669
COTA	0.843	0.870	0.856
CORAL	0.902	0.931	0.916

7.2 Evaluation Results

We first present the overall results of road obstacle detection and classification using a set of optimal parameters, and then study of the parameter selection strategies in the CDRMF and CORAL models.

7.2.1 Road Obstacle Detection Results

We compare the overall accuracy of different methods in Table 2. We can see that our CDRMF method achieves an F1-score of 0.942 (precision=0.953 and recall=0.931), outperforming the other baseline methods. In particular, the TFBOY method fails to detect most of the road obstacles, since the traffic volume decrease induced by road obstacles are overwhelmed by the global decrease of traffic volume during post disaster periods. The ARIMA method achieves a relatively low recall but high precision, meaning that it fails to detect some of the road obstacles (false negatives) but it does not have many wrong detections (false positives), neither. The probable reason is that ARIMA does not model the spatio-temporal collectiveness and thus fails to capture collective anomalies that are not obvious from the view of a single road segment. The DRMF method, on the other hand, achieves relatively low precision and high recall, which means that it detects many road obstacles but only some of them are present in the ground truth set (true positives). This is reasonable since DRMF does not impose structural constraints on the anomalies and thus results in many isolated anomalies that should not be considered being induced by road obstacles. In general, our method successfully captures the collective anomalies induced by road obstacles in disaster response scenario and achieves relatively high detection accuracy.

7.2.2 Road Obstacle Classification Results

We present the road obstacle classification results in Table 3. The ST-ANN method achieves the highest precision and recall using both spatio-temporal features and a *full* label set. However, in practice, collecting such a training set is labor-intensive and time-consuming, which hinders the online deployment in disaster response scenarios. For the other methods, we start from an initial label set of size 7, and limit the total number of labels to be 20. The SCAL and TCAL baseline methods do not perform well, justifying the assumption that neither set of features are significant enough for building an effective road obstacle classifier. In contrast, the COTA baseline performs better by exploiting both sets of features in a co-training model. The proposed CORAL method further improves the performance by incorporating the active-learning diagram, achieving an F1-score of 0.916 with precision=0.902 and recall=0.931, outperforming the other semi-supervised-learning-based baseline methods, and achieving comparable accuracy ST-ANN method using only 12.5% of labels.

7.2.3 Parameter Study

We discuss the parameter selection in the CDRMF and CORAL models as follows.

Low-rank constraint k: in the CDRMF model, the rank constraint parameter k needs to be carefully selected in order to separate the regular patterns from the mixed slow motion behaviors. We perform a rank estimation on M using an SVD-shrinkage method [54], and select $k = 6$ in our experiments that preserve most of the significant singular values of M.

Sparsity constraint c: the sparsity constraint in the CDRMF model determines the number of collective anomalies that can be detected, and thus influences the precision and recall of the model. Based on [54], we vary

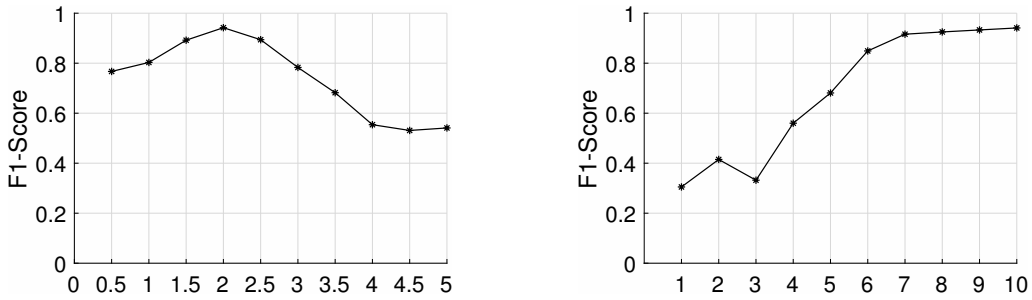

(a) Sparsity constraint c in the CDRAM model

(b) Initial label set size $|G_1|$ in the CORAL model

Fig. 8. Parameter impact analysis and optimal parameter selection.

c from 0 to 5% of the size of M, and present the F1-score under different c values in Figure 8(a). We can see that a sparsity constraint too small or too large may result in suboptimal model accuracy, and thus we select $c = 2\%$ in our experiments.

Initial label set size $|G_1|$: in the CORAL model, the set of initially labeled instances is of great importance for iterative model training. A large initial label set can help achieve high classification accuracy, however collecting these labeled instances requires great effort and reduces the feasibility of online deployment. Therefore, we have to make trade-offs between performance and feasibility. As shown in Figure 8(b), we study the F1-score of the CORAL method against various $|G_1|$ values. We can see that an initial training set of size 7 is large enough to obtain an F1-score higher than 90%. Therefore, we select $|G_1| = 7$ as the optimal initial training set size in our following experiments.

Furthermore, we determine the optimal distance threshold $\delta_p = 1m$ for the slow motion sequence extraction algorithm, which yields closest results to the observations over a series of repeated experiments. In the CORAL model, we empirically set the number of the selected instances $N_c = Na = 2$ based on repeated experiments.

7.2.4 *Runtime Performance*

We implement the CDRMF and CORAL algorithms using Matlab, based on the DRMF matlab package provided by [54]. We deploy our framework on a server with Intel core i7-6700K CPU and 16GB RAM, and it takes an average of 6.1 seconds and 3.2 seconds to do one round of road obstacle detection and classification[11], respectively.

7.3 Case Studies

We conduct case studies on road obstacles identification after the landfall of Typhoon Meranti in Xiamen from 09/15/2016 to 09/17/2016. Figure 9 shows the overall distribution of the detected and classified road obstacles. In general, we observe several water ponds formed in the lower center part of the island, which corresponds to the downtown area with relatively low elevation. Fallen trees block some of the major roads and cause serious transportation problems. Traffic accidents induced by heavy rains and limited visibility increase significantly in complicated road interactions and tunnel entries. These road obstacles pose great challenges for disaster response, and thus need to be identified and removed as early as possible. In the following analysis, we present two cases of identified road obstacles.

7.3.1 *Fallen Trees on Xianyue Expressway*

Figure 9(b) shows the identified fallen trees in Xianyue Expressway, one of the busiest high-capacity road in Xiamen City. Our framework successfully identifies the road obstacle in 3 neighboring road segments at

[11]We do not count in the extra time of the crowdsensing tasks

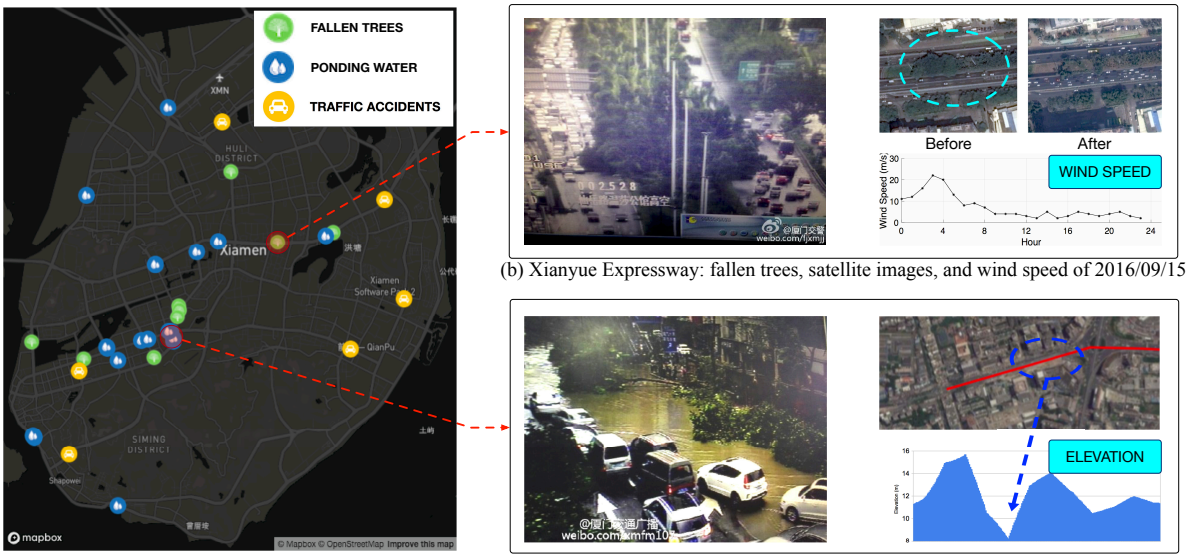

(a) Identified road obstacles during Typhoon Meranti

(b) Xianyue Expressway: fallen trees, satellite images, and wind speed of 2016/09/15

(c) Hubin South Road: ponding water, satellite images, and elevation of the road segment

Fig. 9. Case studies on road obstacle identification after Typhoon Meranti's landfall in Xiamen.

2016/09/15 17:00, which is 16 hours ahead of the event report on the Weibo account of Xiamen Traffic Police[12]. As we can see in Figure 9(b), the road segments were covered by flourishing trees before the typhoon strike, which posed potential risks of fallen trees during the strong winds brought by Typhoon Meranti. Our framework and analysis can not only help urban transportation authorities to clear the obstacles in a timely manner, but also provide decision support for urban environment authorities in roadside tree planning and pruning[51].

7.3.2 *Ponding Waters on Hubin South Road*

Figure 9(c) illustrates the identified ponding water on the surface of Hubin South Road, which is the trunk road in downtown with a relatively low-elevation (Hubin means lakeside). We identified 5 road segments along the road influenced by ponding water at 2016/09/15 08:30, which is 2 hours earlier than the event is reported on the news[13]. From Figure 9(c), we can see several low-lying road segments alone Hubin South Road near the Yundang Lake, which are potentially vulnerable to the heavy rains brought by Typhoon Meranti. With the real-time information at hand, the urban authorities could take preventive actions, for example, by sending out crews to drain the ponding water and prevent further security issues on the road.

8 RELATED WORK

8.1 Disaster Response

Disaster response is the second phase of the disaster management cycle [38], which consists of a set of actions conducted to save lives and prevent further property damage in the post-disaster periods [1, 38]. With the development of mobile Internet technologies and ubiquitous sensing diagrams [57], various approaches have been proposed to help urban authorities take efficient and effective actions in disaster response. For example, Fan et al. [21, 22] proposed to detect and predict the human mobility patterns in earthquakes from large-scale mobile

[12]http://weibo.com/1976447603/E8vIamwnv
[13]http://weibo.com/1750354532/E8lY2Etxr

phone GPS dataset, while Sakaki et al. proposed a real-time earthquake detection method by using Twitter users as social sensors. These knowledge can provide decision supports for urban authorities in disaster response.

In disaster response, restoring the transportation network is usually considered the first step [24, 49], since road network disruptions impede timely rescue, evacuation, and supply [49]. In order to evaluate the post-disaster transportation system performance, Chang et al. [9] develop various transportation quality and accessibility indicators in a quantitative approach. To improve the post-disaster transportation accessibility, Aksu et al. [49] propose a dynamic-path-based mathematical model to clear critical road obstacles in an optimal order with limited resources. However, few works in the transportation research area have addressed the problem of identifying road obstacles in disaster response scenarios.

8.2 Road Obstacle Detection

The road obstacle detection problems have been studied by the computer vision community using several vision-based approaches [34, 35, 52]. For example, LeCun et al. [34] proposed a convolution neural network-based approach to detect road obstacles from videos captured by vehicle's on-board camera, and Lefaix et al. [35] used a vehicle-mounted camera to detect and track road obstacles by analyzing the image motion patterns. However, deploying these vision-based solutions to a large crowd of vehicles requires extremely high cost and thus are infeasible for large-scale road obstacle detection, especially in disaster response scenarios. Another approach for road obstacle detection can be inspired by the existing traffic accident reporting systems, where citizens voluntarily report to the traffic police and media outlets about observed road obstacles using phone calls, social networks, etc. However, the processing of these reports include cross-validating the sources, labeling the locations and scopes on the map, and broadcasting the message back to drivers. Such a process can still be labor intensive and time consuming.

In this paper, we propose to exploit vehicle's GPS trajectories to detect road obstacles based on the abnormal motion behaviors induced by obstacles. In many cities, operational vehicles including taxicabs and buses are required to install GPS trackers and continually report their positions [4]. By collecting and analyzing the vehicle GPS trajectories, a series of urban computing [63] problems have been extensively studied, including route optimization and planning for taxis [37], bikes[14, 16, 17], and buses [11], abnormal trajectory detection [10], city function area studies [40], urban event detection[13], crowdsensing [27, 53] and package delivery [12], etc. Yet, few works have been done in the literature to extract the fine-grained motion behaviors from vehicle trajectories. Instead, such microscopic motion behaviors are extracted from vehicle mounted sensing devices, such as on-board diagnostics (OBD) devices [58], accelerometer-enabled smartphones [19], and driving surveillance cameras [41]. However, these specialized devices are not as widely deployed as GPS trackers in a city-wide level, and thus it is more difficult to obtain large enough datasets for collective vehicle motion analytics.

8.3 Robust Matrix Factorization

In the road obstacle detection phase, we use a robust matrix factorization (RMF) model [3, 29] to separate regular and anomalous components apart from a mixed matrix. RMF models have been widely used in robust modeling and anomaly detection problems [47], such as video background modeling [3], robust face recognition [18], singing voice separation [28], and image denoising [46]. Traditional methods to solve the RMF problem is via relaxation techniques, for example, by exploiting the ℓ_1 norm [46] and $\ell_{2,1}$ norm [29] to approximate the matrix cardinality. In this paper, we use the recent proposed Direct RMF [54] approach instead of relaxation techniques, and inject a clustering step in the optimization process.

8.4 Co-Training and Active Learning

In the road obstacle classification phase, we combine the co-training and active learning diagrams in the CORAL model. Co-training is proposed in [2] as a multi-view learning diagram, and has been used in spatial-temporal modeling [62] and email classification [31], etc. A comprehensive survey on active learning can be found in [45], and the application scenarios of active learning include recommender systems [42], sparse mobile crowdsensing [50], etc. In this work, we combine both co-training and active learning diagrams to address the challenges of heterogeneous features and sparse labels.

9 CONCLUSION

In this paper, we propose a two-phase framework to detect and classify road obstacles in disaster response scenarios, leveraging large-scale vehicle trajectories and many cross-domain urban sensing datasets. In order to detect road obstacles, we extract slow motion behaviors from vehicle trajectories, and propose the CDRMF approach to detect collective anomalies from a mixture of slow motion behaviors, and correspond them to road obstacles. In order to recognize the types of the detected obstacles, we exploit the spatio-temporal contextual features extracted from various environment sensing data to train a classification model. To address the challenges of heterogeneous features and insufficient labels, we propose a semi-supervised approach combining co-training and active learning. We evaluate our framework using real-world datasets collected from Xiamen City. Results show that our framework accurately detects and classifies the road obstacles in the 2016 typhoon season with an overall accuracy both above 90%, and outperforms the baseline methods.

In the future, we intend to improve this work from the following aspects. First, we plan to use trajectories of various kinds of vehicles besides taxis, such as buses and rental cars. Second, we plan to characterize the slow motion behaviors in a finer granularity, for example, by identifying waiting and turning behaviors. Third, we plan to improve the granularity of road spatial features by incorporating the high-resolution LIDAR (Light Detection and Ranging) data collected by our team in Xiamen University for better classification of road obstacles. Fourth, we plan to evaluate our framework in other cities with different geographic and meteorological settings, and explore the obstacle identification problem under other nature disaster types.

10 ACKNOWLEDGMENT

We would like to thank the reviewers and editors for their constructive suggestions. This research was supported by the China Fundamental Research Funds for the Central Universities No. 0630/ZK1074, NSF of China No. U1605254, No. 61371144, No. 61772460, No. 61300232, and No. 61772136.

REFERENCES

[1] G. Barbarosoglu and Y. Arda. 2004. A Two-Stage Stochastic Programming Framework for Transportation Planning in Disaster Response. *Journal of the Operational Research Society* 55, 1 (2004), 43–53.
[2] Avrim Blum and Tom Mitchell. 1998. Combining Labeled and Unlabeled Data with Co-Training. In *Proceedings of the Eleventh Annual Conference on Computational Learning Theory (COLT'98)*. ACM, 92–100.
[3] Emmanuel J. Candès, Xiaodong Li, Yi Ma, and John Wright. 2011. Robust Principal Component Analysis? *J. ACM* 58, 3 (2011), 1:37.
[4] Pablo Samuel Castro, Daqing Zhang, Chao Chen, Shijian Li, and Gang Pan. 2013. From Taxi GPS Traces to Social and Community Dynamics: A Survey. *ACM Computer Survey* 46, 2 (2013), 17:1–17:34.
[5] Centre for Research on the Epidemiology of Disasters. 2015. *The Human Cost of Natural Disasters 2015: A Global Perspective*. Technical Report. UN Office for Disaster Risk Reduction, Geneva, Switzerland.
[6] P. K. Chan and M. V. Mahoney. 2005. Modeling Multiple Time Series for Anomaly Detection. In *Proceedings of the Fifth IEEE International Conference on Data Mining (ICDM'05)*. ACM, 8–16.
[7] Varun Chandola, Arindam Banerjee, and Vipin Kumar. 2009. Anomaly Detection: A Survey. *ACM Computer Survey* 41, 3 (2009), 1–58.
[8] Chih-Chung Chang and Chih-Jen Lin. 2011. LIBSVM: A Library for Support Vector Machines. *ACM Transactions on Intelligent Systems and Technology* 2, 3 (2011), 1–27.

[9] Stephanie E Chang and Nobuoto Nojima. 2001. Measuring Post-Disaster Transportation System Performance: The 1995 Kobe Earthquake in Comparative Perspective. *Transportation Research Part A: Policy and Practice* 35, 6 (2001), 475–494.

[10] C. Chen, D. Zhang, P.S. Castro, N. Li, L. Sun, S. Li, and Z. Wang. 2013. iBOAT: Isolation-Based Online Anomalous Trajectory Detection. *IEEE Transactions on Intelligent Transportation Systems* 14, 2 (2013), 806–818.

[11] Chao Chen, Daqing Zhang, Nan Li, and Zhi-Hua Zhou. 2014. B-Planner: Planning Bidirectional Night Bus Routes Using Large-Scale Taxi GPS Traces. *IEEE Transactions on Intelligent Transportation Systems* 15, 4 (2014), 1451–1465.

[12] C. Chen, D. Zhang, X. Ma, B. Guo, L. Wang, Y. Wang, and E. Sha. 2017. Crowddeliver: Planning City-Wide Package Delivery Paths Leveraging the Crowd of Taxis. *IEEE Transactions on Intelligent Transportation Systems* 18, 6 (2017), 1478–1496.

[13] L. Chen, J. Jakubowicz, D. Yang, D. Zhang, and G. Pan. 2017. Fine-Grained Urban Event Detection and Characterization Based on Tensor Cofactorization. *IEEE Transactions on Human-Machine Systems* 47, 3 (2017), 380–391.

[14] Longbiao Chen, Xiaojuan Ma, Thi-Mai-Trang Nguyen, Gang Pan, and Jérémie Jakubowicz. 2016. Understanding Bike Trip Patterns Leveraging Bike Sharing System Open Data. *Frontiers of Computer Science* (2016), 1–11.

[15] L. Chen, D. Zhang, X. Ma, L. Wang, S. Li, Z. Wu, and G. Pan. 2016. Container Port Performance Measurement and Comparison Leveraging Ship GPS Traces and Maritime Open Data. *IEEE Transactions on Intelligent Transportation Systems* 17, 5 (2016), 1227–1242.

[16] Longbiao Chen, Daqing Zhang, Gang Pan, Xiaojuan Ma, Dingqi Yang, Kostadin Kushlev, Wangsheng Zhang, and Shijian Li. 2015. Bike Sharing Station Placement Leveraging Heterogeneous Urban Open Data. In *Proceedings of the ACM International Joint Conference on Pervasive and Ubiquitous Computing*, Vol. UbiComp'15. ACM, 571–575.

[17] Longbiao Chen, Daqing Zhang, Leye Wang, Dingqi Yang, Xiaojuan Ma, Shijian Li, Zhaohui Wu, Gang Pan, Thi-Mai-Trang Nguyen, and Jérémie Jakubowicz. 2016. Dynamic Cluster-Based Over-Demand Prediction in Bike Sharing Systems. In *Proceedings of the ACM International Joint Conference on Pervasive and Ubiquitous Computing (UbiComp'16)*. ACM, 841–852.

[18] L. Du, X. Li, and Y. D. Shen. 2012. Robust Nonnegative Matrix Factorization via Half-Quadratic Minimization. In *Proceedings of the 12th IEEE International Conference on Data Mining (ICDM'12)*. IEEE, 201–210.

[19] H. Eren, S. Makinist, E. Akin, and A. Yilmaz. 2012. Estimating Driving Behavior by a Smartphone. In *Proceedings of the IEEE Intelligent Vehicles Symposium*. IEEE, 234–239.

[20] Levi Ewan, Ahmed Al-Kaisy, and David Veneziano. 2013. Remote Sensing of Weather and Road Surface Conditions. *Transportation Research Record: Journal of the Transportation Research Board* 2329 (July 2013), 8–16.

[21] Zipei Fan, Xuan Song, and Ryosuke Shibasaki. 2014. CitySpectrum: A Non-Negative Tensor Factorization Approach. In *Proceedings of the ACM International Joint Conference on Pervasive and Ubiquitous Computing (UbiComp'14)*. ACM, 213–223.

[22] Zipei Fan, Xuan Song, Ryosuke Shibasaki, and Ryutaro Adachi. 2015. CityMomentum: An Online Approach for Crowd Behavior Prediction at a Citywide Level. In *Proceedings of the ACM International Joint Conference on Pervasive and Ubiquitous Computing (UbiComp '15)*. ACM, 559–569.

[23] Tom Fawcett. 2006. An Introduction to ROC Analysis. *Pattern Recognition Letters* 27, 8 (2006), 861–874.

[24] FEMA. 2007. *Public Assistance: Debris Management Guide.* Technical Report. Federal Emergency Management Agency, Washington, DC.

[25] Nir Friedman, Dan Geiger, and Moises Goldszmidt. 1997. Bayesian Network Classifiers. *Machine Learning* 29, 2-3 (1997), 131–163.

[26] G. H. Golub and C. Reinsch. 1970. Singular Value Decomposition and Least Squares Solutions. *Numer. Math.* 14, 5 (1970), 403–420.

[27] B. Guo, C. Chen, D. Zhang, Z. Yu, and A. Chin. 2016. Mobile Crowd Sensing and Computing: When Participatory Sensing Meets Participatory Social Media. *IEEE Communications Magazine* 54, 2 (2016), 131–137.

[28] Ying Hu and Guizhong Liu. 2015. Separation of Singing Voice Using Nonnegative Matrix Partial Co-Factorization for Singer Identification. *IEEE/ACM Transactions on Audio, Speech, and Language Processing* 23, 4 (2015), 643–653.

[29] Jin Huang, Feiping Nie, Heng Huang, and Chris Ding. 2014. Robust Manifold Nonnegative Matrix Factorization. *ACM Transactions on Knowledge Discovery from Data* 8, 3 (2014), 1–21.

[30] Yangqing Jia, Evan Shelhamer, Jeff Donahue, Sergey Karayev, Jonathan Long, Ross Girshick, Sergio Guadarrama, and Trevor Darrell. 2014. Caffe: Convolutional Architecture for Fast Feature Embedding. In *Proceedings of the 22nd ACM International Conference on Multimedia (MM'14)*. ACM, 675–678.

[31] Svetlana Kiritchenko and Stan Matwin. 2011. Email Classification with Co-Training. In *Proceedings of the 2011 Conference of the Center for Advanced Studies on Collaborative Research (CASCON '11)*. IBM Corp., 301–312.

[32] T. Kolda and B. Bader. 2009. Tensor Decompositions and Applications. *SIAM Rev.* 51, 3 (2009), 455–500.

[33] Nicholas D. Lane, Petko Georgiev, and Lorena Qendro. 2015. DeepEar: Robust Smartphone Audio Sensing in Unconstrained Acoustic Environments Using Deep Learning. In *Proceedings of the ACM International Joint Conference on Pervasive and Ubiquitous Computing (UbiComp'15)*. ACM, 283–294.

[34] Yann LeCun, Urs Muller, Jan Ben, Eric Cosatto, and Beat Flepp. 2005. Off-Road Obstacle Avoidance Through End-to-End Learning. In *Proceedings of the 18th International Conference on Neural Information Processing Systems (NIPS'05)*. 739–746.

[35] G. Lefaix, T. Marchand, and P. Bouthemy. 2002. Motion-Based Obstacle Detection and Tracking for Car Driving Assistance. In *Proceedings of the 16th International Conference on Pattern Recognition*, Vol. 4. IEEE, 74–77.

[36] Jing Lei. 2014. Classification with Confidence. *Biometrika* 101, 4 (2014), 755–769.

[37] Bin Li, Daqing Zhang, Lin Sun, Chao Chen, Shijian Li, Guande Qi, and Qiang Yang. 2011. Hunting or Waiting? Discovering Passenger-Finding Strategies from a Large-Scale Real-World Taxi Dataset. In *Proceedings of the IEEE International Conference on Pervasive Computing and Communications Workshops (PerCom'11 Workshops)*. IEEE, 63–68.
[38] David A. McEntire. 2014. *Disaster Response and Recovery: Strategies and Tactics for Resilience.* John Wiley & Sons.
[39] Kamal Nigam and Rayid Ghani. 2000. Analyzing the Effectiveness and Applicability of Co-Training. In *Proceedings of the 9th International Conference on Information and Knowledge Management (CIKM '00)*. ACM, 86–93.
[40] G. Pan, G. Qi, Z. Wu, D. Zhang, and S. Li. 2013. Land-Use Classification Using Taxi GPS Traces. *IEEE Transactions on Intelligent Transportation Systems* 14, 1 (2013), 113–123.
[41] Thomas A. Ranney. 1994. Models of Driving Behavior: A Review of Their Evolution. *Accident Analysis & Prevention* 26, 6 (1994), 733–750.
[42] Neil Rubens, Mehdi Elahi, Masashi Sugiyama, and Dain Kaplan. 2015. Active Learning in Recommender Systems. In *Recommender Systems Handbook*. Springer, 809–846.
[43] N. Rusli, M. R. Majid, and A. H. M. Din. 2014. Google Earth's Derived Digital Elevation Model: A Comparative Assessment with Aster and SRTM Data. *IOP Conference Series: Earth and Environmental Science* 18, 1 (2014), 12–65.
[44] Jörg Sander, Martin Ester, Hans-Peter Kriegel, and Xiaowei Xu. 1998. Density-Based Clustering in Spatial Databases: The Algorithm Gdbscan and Its Applications. *Data Mining and Knowledge Discovery* 2, 2 (1998), 169–194.
[45] Burr Settles. 2010. *Active Learning Literature Survey.* Technical Report. University of Wisconsin.
[46] B. Shen, B. D. Liu, Q. Wang, and R. Ji. 2014. Robust Nonnegative Matrix Factorization via L1 Norm Regularization by Multiplicative Updating Rules. In *Proceedings of the IEEE International Conference on Image Processing (ICIP'14)*. 5282–5286.
[47] P. Sprechmann, A. M. Bronstein, and G. Sapiro. 2015. Learning Efficient Sparse and Low Rank Models. *IEEE Transactions on Pattern Analysis and Machine Intelligence* 37, 9 (2015), 1821–1833.
[48] Nathan Srebro and Adi Shraibman. 2005. Rank, Trace-Norm and Max-Norm. In *Proceedings of the 18th Annual Conference on Learning Theory (COLT'05)*. Springer, 545–560.
[49] Dilek Tuzun Aksu and Linet Ozdamar. 2014. A Mathematical Model for Post-Disaster Road Restoration: Enabling Accessibility and Evacuation. *Transportation Research Part E: Logistics and Transportation Review* 61 (2014), 56–67.
[50] Leye Wang, Daqing Zhang, Animesh Pathak, Chao Chen, Haoyi Xiong, Dingqi Yang, and Yasha Wang. 2015. CCS-TA: Quality-Guaranteed Online Task Allocation in Compressive Crowdsensing. In *Proceedings of the ACM International Joint Conference on Pervasive and Ubiquitous Computing*. ACM, New York, NY, USA, 683–694.
[51] Kathleen L. Wolf. 2006. Urban Trees and Traffic Safety: Considering the U.S. Roadside Policy and Crash Data. *Arboriculture and Urban Forestry* 32, 4 (2006), 170–179.
[52] M. Xie, L. Trassoudaine, J. Alizon, and J. Gallice. 1994. Road Obstacle Detection and Tracking by an Active and Intelligent Sensing Strategy. *Machine Vision and Applications* 7, 3 (1994), 165–177.
[53] H. Xiong, D. Zhang, G. Chen, L. Wang, V. Gauthier, and L. E. Barnes. 2016. iCrowd: Near-Optimal Task Allocation for Piggyback Crowdsensing. *IEEE Transactions on Mobile Computing* 15, 8 (2016), 2010–2022.
[54] L. Xiong, X. Chen, and J. Schneider. 2011. Direct Robust Matrix Factorizatoin for Anomaly Detection. In *Proceedings of the 11th IEEE International Conference on Data Mining (ICDM'11)*. 844–853.
[55] Jar-Ferr Yang and Chiou-Liang Lu. 1995. Combined Techniques of Singular Value Decomposition and Vector Quantization for Image Coding. *IEEE Transactions on Image Processing* 4, 8 (1995), 1141–1146.
[56] Y. Yu, J. Li, H. Guan, C. Wang, and C. Wen. 2016. Bag of Contextual-Visual Words for Road Scene Object Detection From Mobile Laser Scanning Data. *IEEE Transactions on Intelligent Transportation Systems* 17, 12 (2016), 3391–3406.
[57] Daqing Zhang, Bin Guo, and Zhiwen Yu. 2011. The Emergence of Social and Community Intelligence. *Computer* 44, 7 (2011), 21–28.
[58] Minging Zhang, Chao Chen, Tianyu Wo, Tao Xie, Md Zakirul Alam Bhuiyan, and Xuelian Lin. 2017. SafeDrive: Online Driving Anomaly Detection From Large-Scale Vehicle Data. *IEEE Transactions on Industrial Informatics* 13, 4 (2017), 2087–2096.
[59] Yihao Zhang, Junhao Wen, Xibin Wang, and Zhuo Jiang. 2014. Semi-Supervised Learning Combining Co-Training with Active Learning. *Expert Systems with Applications* 41, 5 (2014), 2372–2378.
[60] Yu Zheng. 2015. Trajectory Data Mining: An Overview. *ACM Trans. Intell. Syst. Technol.* 6, 3 (2015), 1–41.
[61] Yu Zheng, Licia Capra, Ouri Wolfson, and Hai Yang. 2014. Urban Computing: Concepts, Methodologies, and Applications. *ACM Trans. Intell. Syst. Technol.* 5, 3 (2014), 1–55.
[62] Yu Zheng, Furui Liu, and Hsun-Ping Hsieh. 2013. U-Air: When Urban Air Quality Inference Meets Big Data. In *Proceedings of the 19th ACM SIGKDD International Conference on Knowledge Discovery and Data Mining (KDD '13)*. ACM, 1436–1444.
[63] Yu Zheng, Yanchi Liu, Jing Yuan, and Xing Xie. 2011. Urban Computing with Taxicabs. In *Proceedings of the ACM International Joint Conference on Pervasive and Ubiquitous Computing (UbiComp'11)*. ACM, 89–98.
[64] Yu Zheng, Huichu Zhang, and Yong Yu. 2015. Detecting Collective Anomalies from Multiple Spatio-Temporal Datasets Across Different Domains. In *Proceedings of the ACM International Conference on Advances in Geographic Information Systems*. ACM, 1–10.

Received August 2017; accepted October 2017